Tetrahedron 68 (2012) 8924–8930

Contents lists available at SciVerse ScienceDirect

Tetrahedron

journal homepage: www.elsevier.com/locate/tet

Synthesis, electrochemistry, and photophysical properties of pyrazolino[60]fullerene–1,8-naphthalimide fluorescent derivatives

Beiqiong Lu [a], Jianmin Zhang [a,c,**], Jia Li [b], Jianhua Yao [b], Minjian Wang [a], Yuanhai Zou [a], Shizheng Zhu [c,*]

[a] Department of Chemistry, School of Science, Shanghai University, No. 99, Shangda Road, Shanghai 200444, China
[b] Department of Computer Chemistry and Chemoinformatics, Shanghai Institute of Organic Chemistry, Shanghai 200032, PR China
[c] Key Laboratory of Organofluorine Chemistry, Shanghai Institute of Organic Chemistry, Chinese Academy of Sciences, Shanghai 200032, PR China

ARTICLE INFO

Article history:
Received 25 May 2012
Received in revised form 2 August 2012
Accepted 10 August 2012
Available online 16 August 2012

Keywords:
Fullerene C_{60}
Electrochemical
Photophysical
Chemical calculation
Pyrazoline

ABSTRACT

A series of pyrazolino[60]fullerene–1,8-naphthalimide (Pz[60]–NI) fluorescent derivatives were synthesized in one pot by a [3+2] dipolar cycloaddition between C_{60} and functionalized hydrazones in good yield. In contrast with 4-aziridino[60]fullerene–1,8-naphtalimide dyads, Pz[60]–NI derivatives present stronger fluorescence intensity. Electrochemical study revealed that Pz[60]–NI presents better electron accepting character than the parent C_{60}. The natural bond orbital of the dyads were calculated using density functional theory method and found that the sp3 nitrogen atom in the pyrazoline ring plays a key role in the charge transfer process.

1. Introduction

The construction of artificial photosynthetic models to mimic natural photosynthesis through the design of covalently linked electron-donor and -acceptor moieties is an area of great interest. The interest lies in the development of efficient organic solar cells[1] and other areas of nanotechnology, such as photonics or sensors.[2] Fullerene C_{60} is an excellent electron acceptor,[3] its visible light absorption allows energy transfer (EN) and electron transfer (ET) in fullerene-donor dyads.[4] These systems can undergo efficient photoinduced electron transfer (PET) processes to give long-lived radical-ion pairs.[2]

Fullerene-fused pentagonal heterocyclic rings, such as fulleroindolines,[5] fullerene-fused lactones,[6] and pyrazolo-fullerenes have been the focus of intense research. For example, pyrazolofullerenes (PzC_{60}) derivatives have recently been used to link electroactive groups to the C_{60} cage and the products showed efficient PET processes.[7] It has been shown that the lone-pair electron of the pyrazoline sp^3 nitrogen atom is able to afford PET to the C_{60} cage.[8] Thus, the Pz moiety acts as an intermediary in the PET process from the donor unit present in the organic addend.[9] Interestingly, recent studies on organic photovoltaic cells[10] constructed with donor polymers and fullerene derivatives as acceptors indicate that cells built with PzC_{60} derivatives have a better efficiency than those constructed with [6,6]-phenyl-C_{61}-butyric acid methyl ester (PCBM), highlighting the interest of these compounds.

We have reported the synthesis of 4-aziridino[60]fullerene–1,8-naphthalimide under microwave irradiation.[11] It is well known that the naphthalimide usually exhibits strong fluorescence on irradiation, which usually acts as supermolecular moieties for the study of PET processes[12] and fluorescence switcher.[13] To our knowledge, the incorporation of bischromophore (pyrazoline and naphthalimide) within C_{60} has rarely been studied. Herein, we present the synthesis, electrochemical properties and molecular

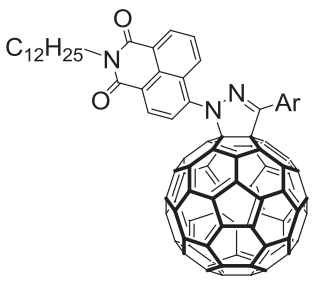

4

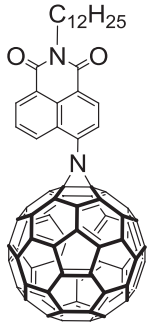

5

* Corresponding author. Tel.: +86 021 5492 5185; fax: +86 021 6416 6128
** Corresponding author. Tel./fax: +86 021 6613 3801; e-mail addresses: lubeiqiong@163.com (B. Lu), jmzhang@shu.edu.cn (J. Zhang), zhusz@mail.sioc.ac.cn (S. Zhu).

0040-4020/$ – see front matter © 2012 Elsevier Ltd. All rights reserved.
http://dx.doi.org/10.1016/j.tet.2012.08.031

orbital calculations of pyrazolino[60]fullerene–1,8-naphtalimide derivatives (Pz[60]–NI) and the first comparative study of the photophysical properties of pyrazolo- (**4a**–**e**) and aziridino–fullerene (**5**) derivatives. The compound **5** is *N*-dodecyl-4-aziridinofullerene–1,8-naphthalimide that was reported by our group.[11]

2. Results and discussion

2.1. Synthesis

The hydrazones **3** were prepared according to the literature method,[14] which was then tried to be introduced to the C_{60} skeleton by a [3+2] dipolar cycloaddition reaction (Scheme 1).[15] As listed in Table 1, the reaction of hydrazone **3c** with C_{60} was chosen as a model reaction to screen the optimized reactions. Initial experiment was performed using $PhI(OAc)_2$ (*Iodobenzene diacetate*) as additive and the reaction was carried out at room temperature in various solvents with various mole ratios of **3c**:$PhI(OAc)_2$:C_{60}. It was found that the yield of product **4c** could be improved by increasing the amount of **3c** and $PhI(OAc)_2$ or C_{60} (entries 2 and 3). Further increasing the amount of **3c** and $PhI(OAc)_2$ had a negligible effect on the product yield. The temperature can affect the yield of product—when temperature was raised to 40 °C in benzene, the yield improved to 85%. However, when the reaction mixture was refluxed in benzene, the yield dropped to 68%. Other solvents, such as toluene and *o*-DCB were also evaluated in various temperatures (entries 4 and 5). [hydroxyl(tosyloxy)iodo]benzene (HTIB) was used as additive to mediate the reaction, but the yield was smaller than that when $PhI(OAc)_2$ was used (entry 7). After optimizations, the best reaction conditions for the preparation of Pz[60]–NI were ascertained as 1 equiv of C_{60}, 2 equiv **3**, 2 equiv $PhI(OAc)_2$ in benzene at 40 °C under nitrogen atmosphere (entry 6).

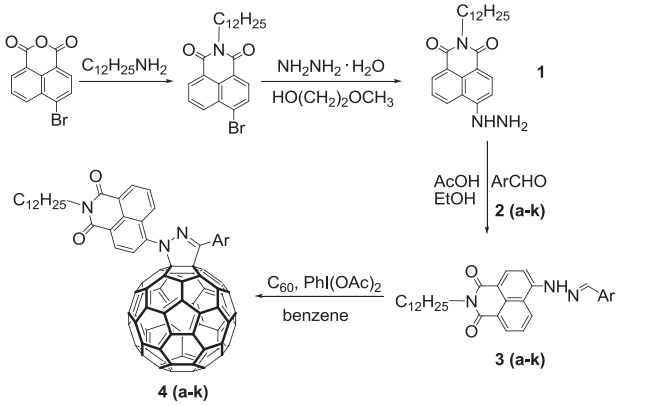

Scheme 1. Preparation of Pz[60]–NI derivatives.

Having established suitable reaction conditions, a serious of Pz[60]–NI derivatives **4** were prepared. As shown in Table 2, most examined substrates **3** provided good yields of 70–86%, except **4e** and **4k** with 67% and 66% yields, respectively.

The structures of the Pz[60]–NI products **4a**–**k** were established by spectroscopic methods (UV–vis, FTIR, ^1H, ^{19}F, ^{13}C NMR, and ESI mass). The mass spectra of the product **4** exhibited the expected $[M-H]^-$ peaks matching the calculated molecular weights. The ^1H NMR spectra of **4** in $CDCl_3$ exhibited similar signals to the hydrazones **3** and were shifted slightly to the downfield. The ^1H NMR spectrum of **4a** displayed one doublet and one multiplet at 8.33 (d, 2H) and 7.52–7.55 (m, 3H) for the phenyl ring and five singlets at 9.14, 8.74, 8.66, 8.27, and 7.83 ppm for the NI moiety. 4.17 (t, 2H), 1.72–1.73 (m, 2H), 1.25 (s, 18H), and 0.87 (m, 3H) belong to the alkyl group ($C_{12}H_{25}$–). The observed signals in the ^{13}C NMR spectra were in agreement with the proposed structures, showing that PzC_{60}–NI derivatives were [6,6]-closed isomers. In the ^{13}C NMR spectrum of **4a** there were 37 peaks in the range of 119–164 ppm due to the sp^2 carbons of the C_{60} skeleton, NI moiety and phenyl ring. Two peaks at about 60.42 and 58.50 ppm for the two sp^3 carbons of the C_{60}. The two peaks at 163.80 and 164.14 were attributed to the two C=O, one peak at 147.67 ppm was related to the C=N carbon atom.

Table 1
Optimization of reaction conditions of C_{60} with **3c**

Entry	Mole ratio[a]	Solvent	Temperature (°C)	Time (min)	Yield[b] (%)	Isolated yield (%)	Recovered C_{60} (%)
1	1:1:1	Benzene	RT	50	55	8	80
2	1:1:3	Benzene	RT	50	80	19	74
3	2:2:1	Benzene	RT	50	82	21	72
4	2:2:1	Toluene	RT	50	66	15	75
5	2:2:1	*o*-DCB	RT	50	80	8	84
6	2:2:1	Benzene	40	50	85	23	74
7[c]	2:2:1	Benzene	40	30	61	9	76
8	2:2:1	Benzene	60	30	76	16	73
9	2:2:1	Benzene	80	30	68	10	75

RT: room temperature.
[a] Mole ratio refers to **3c**:$PhI(OAc)_2$:C_{60}.
[b] Isolated yield based on the reacted C_{60}.
[c] Two equiv of HTIB was used as additive.

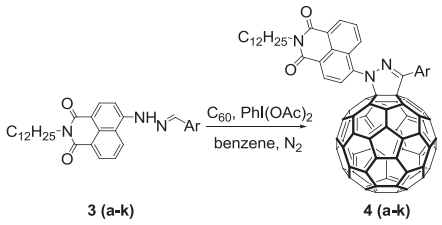

Table 2
Preparation of various Pz[60]–NI derivatives

Entry	Ar of reactant **3**	Product **4**[a]	Yield[b] (%)	Isolated yield (%)	Recovered C_{60} (%)
1	C_6H_5	4a	81	24	68
2	C_6F_5	4b	83	21	75
3	4-$NO_2C_6H_4$	4c	85	23	74
4	4-$Me_2NC_6H_4$	4d	70	22	68
5	4-$EtOC_6H_4$	4e	67	21	69
6	4-FC_6H_4	4f	83	23	72
7	4-ClC_6H_4	4g	85	27	65
8	4-BrC_6H_4	4h	86	29	66
9	2,4-$2FC_6H_3$	4i	82	24	70
10	4-CNC_6H_4	4j	80	25	69
11	4-$OHCC_6H_4$	4k	66	22	67

[a] Mole ratio refers to **3**: $PhI(OAc)_2$:C_{60}=2:2:1; under nitrogen atmosphere; all reactions were performed in benzene at 40 °C.
[b] Isolated yield based on the reacted C_{60}.

2.2. UV–vis spectra

The UV–vis spectra of dyads **3**(**a**,**b**,**e**), **4**(**a**,**b**,**e**) and **5** in $CHCl_3$ at room temperature are shown in Fig. 1. The UV–vis spectra of **4**(**a**,**b**,**e**) and **5** were similar—two main absorption peaks appearing at about 254 and 326 nm. Both of them were the characteristic of the C_{60} moiety. A peak at 390 nm was observed in **5**, which attributes to NI moiety. The most distinct difference of **3**(**a**,**b**,**e**) was the main absorption peak at 420–460 nm, which attributes to NI moiety. Moreover, the intensity of this peak was varying from **3a**

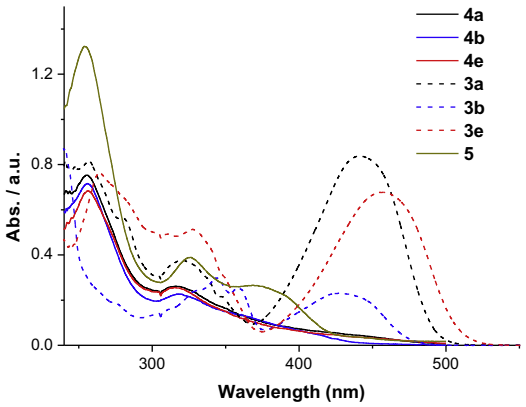

Fig. 1. UV–vis spectra of **3**(**a**,**b**,**e**), **4**(**a**,**b**,**e**) and **5** in $CHCl_3$ solutions at room temperature (c=7×10^{-6} mol/L).

and **3e** to **3b**, as the increasing of electronic deficiency of the substituent R. While in **4**(**a**,**b**,**e**) this peak disappeared, the observation suggests that the UV–vis spectra of **4**(**a**,**b**,**e**) are more likely to be the characteristic of C_{60} than that of NI moiety.

2.3. Fluorescence spectra

Fluorescence spectra of corresponding hydrazones **3**(**a**,**b**,**e**), **4**(**a**,**b**,**e**), and **5** were measured in $CHCl_3$, as shown in Fig. 2. The fluorescence peaks of **4**(**a**,**b**,**e**) were observed at 430–440 nm while the peak of **5**, appearing at 495 nm, was similar to the appended donor NI moiety's emission band. The fluorescence intensity of **5** was decreased approximately 12-folds than that of **4a**. The C=N double bonds and sp^3 nitrogen atom of pyrazoline ring make charge transmitting easier than aziridine ring, so we inferred that pyrazoline ring acts as a better bridge than aziridine ring in terms of a PET process. The fluorescence peaks of hydrazones were observed at 493–537 nm and as the increasing of electronic deficiency of the substituent R, the fluorescence intensities were varying considerably from **3a** and **3e** to **3b**. The fluorescence peak for **4**(**a**,**b**,**e**) were blue-shifted by 60–100 nm relative to the corresponding hydrazones, and the fluorescence intensities of **4** were significantly quenched. On one hand, the new formed pyrazoline ring blocked charge transferring and changed conjugation system, On the other hand, a charge-transfer interaction in the excited state between the C_{60} moiety and the appended donor NI moiety. As the electronic deficiency of the substituent increased, the fluorescence intensity of dyads **4** became weaker (i.e., **4e**>**4b**).

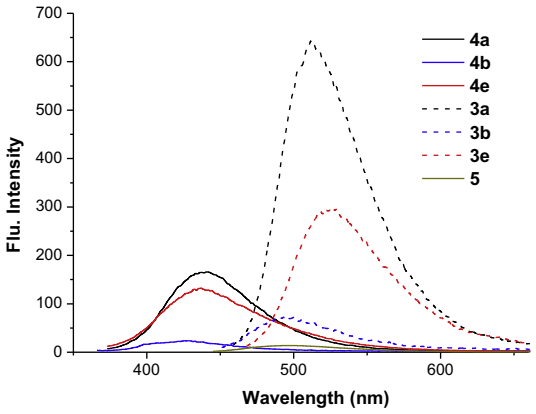

Fig. 2. Fluorescence spectra of **3**(**a**,**b**,**e**), **4**(**a**,**b**,**e**) and **5** solutions in $CHCl_3$ at room temperature (c=7.0×10^{-6} mol/L).

2.4. Electrochemical examinations

The results of the cyclic voltammetry (CV) studies are summarized in Table 3. In Fig. 3 product **4e** show a quasi-reversible electrochemical behavior with four one-electron reduction waves corresponding to the reduction of the C_{60} moiety and the organic addend hydrazones **3**. Dyads **4**(**a**–**d**) showed similar shape to the **4e**. In this case, the first reduction potential values exhibit an anodic shift (80 mV for **4c** and 60 mV for **4b**), in comparison with the parent C_{60}. Especially, when the substituent R on the phenyl ring was more electron-withdrawing, the first reduction potentials shift to more positive values. We attributed this shift to the electronegative character of the nitrogen atom linked to the C_{60} core. Therefore, dyads **4** present better acceptor ability than parent C_{60}. An irreversible oxidation wave at around 0.58 V, corresponding to the oxidation of the hydrazones **3**, was also observed.

Table 3
Redox potentials of organofullerenes **4**(**a**–**e**) and **3**(**a**–**e**)

Compound	Red_4/V	Red_3/V	Red_2/V	Red_1/V	Ox_1/V
C_{60}	−2.55	−2.07	−1.59	−1.12	
4a	−2.26	−2.05	−1.58	−1.08	0.57
3a	−2.27		−1.61		0.55
4b	−2.28	−1.90	−1.55	−1.06	0.54
3b	−2.40	−1.94	−1.58		0.60
4c	−2.17	−1.87	−1.52	−1.04	0.53
3c	−2.31		−1.59		0.64
4d	−2.28	−1.89	−1.55	−1.08	0.55
3d			−1.61		0.68
4e	−2.35	−2.06	−1.61	−1.10	0.63
3e			−1.66		0.67

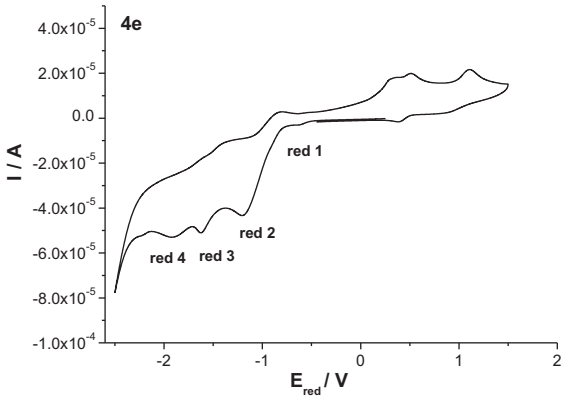

Fig. 3. Cyclic voltammogram of product **4e**.

2.5. Molecular orbital calculations

To observe an insight into the molecular structures, theoretical calculations within density functional theory (DFT) framework were performed at the B3LYP/6-31G level.[16,17] The optimized structures of **4a** and **4b** are shown in Fig. 4. For **4a** and **4b**, the two

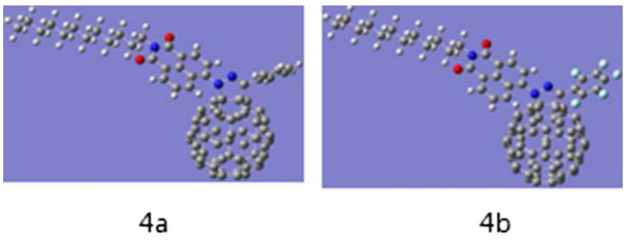

Fig. 4. Fully optimized structures of **4a** and **4b**.

donor moieties are aligned in an L-shape with an angle of approximately 90° between the two units. The center-to-center distances (Rcc) between C_{60} and the donor entities were estimated to be 8.006 and 8.036 Å for **4a** and **4b**, respectively. In **4a**, the NI moiety was twisted by 47.7° with respect to the pyrazoline ring, whereas the phenyl group was twisted by 53.8°. In **4b**, the NI moiety was twisted by 50.5° with respect to the pyrazoline ring, whereas the pentafluorophenyl was twisted by 86.9°.

The highest occupied molecular orbital (HOMO) and lowest unoccupied molecular orbital (LUMO) of **4a** and **4b** are shown in Fig. 5. The electron density of the HOMO was found to be delocalized among the NI moiety and pyrazoline ring, whereas the electron density of the LUMO was located in the C_{60} cage. These results suggest the existence of charge-separated states having a structure like $(NI)Pz^{+}{=}C60^{-}$.[18] The electron was localized on the C_{60} sphere, and the radical cation was delocalized along the NI moiety and Pz groups.

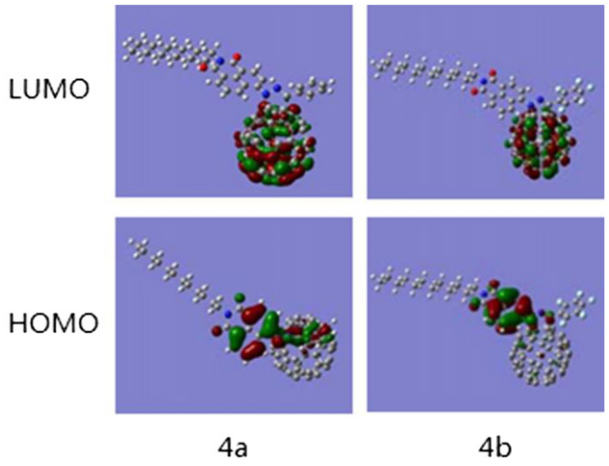

Fig. 5. The HOMO and LUMO of **4a** and **4b**.

As shown in Table 4, the HOMO energy levels of **4a**–**e** are higher in energy relative to parent C_{60} (−9.48 eV). The LUMO energy levels of these systems **4a**–**e** are lower than that of C_{60} (−2.88 eV). Consequently, these systems present a small HOMO–LUMO gap, enabling an easier electron-transfer process, particularly in the case of **4d** (5.41 eV).To explain the charge transfer process, the natural bond orbital (NBO) of **3**(**a**,**b**) and **4**(**a**,**b**) were calculated. Fig. 6 represents the model of dyads **3**(**a**,**b**) and **4**(**a**,**b**). The results are summarized in Table 5, which show that after hydrazones **3** fused with C_{60}, the positive charges of NI moiety were significantly increased. In Pz groups, the positive charges of N5 increased to 0.034 for **4a** and 0.038 for **4b**, while the positive charges of C6 increased 0.209 for **4a** and 0.223 for **4b**. We inferred that the sp^3 nitrogen atom of N5 had stronger charge transmission ability than C6; therefore, NI moiety donated more charges to the C_{60} moiety than to substituted aryl. Moreover, the fluorescence intensity and atomic charges behaved certain correlation. In Table 5, the positive charges of C6 and C11 increased, especially when the substituted aryl was pentafluorophenyl, **4b** acquired more positive charges than **4a**.

Table 4
The LUMO and HOMO energies and LUMO–HOMO energy gaps (Eg) were calculated by PM3 level

Compound	E_{HOMO} (eV)	E_{LUMO} (eV)	Eg (eV)
C_{60}	−9.48	−2.88	6.59
4a	−9.16	−3.28	5.87
4b	−9.28	−3.39	5.88
4c	−9.34	−3.46	5.87
4d	−8.65	−3.23	5.41
4e	−9.13	−3.25	5.87

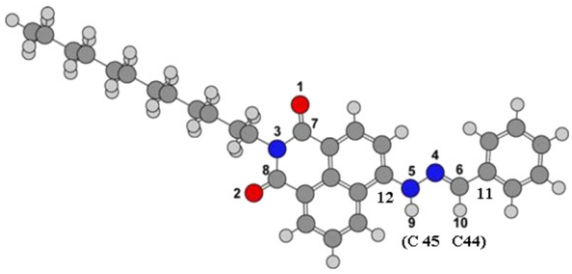

Fig. 6. The model of dyads **3**(**a**,**b**) and **4**(**a**,**b**) for NBO calculation.

Table 5
The atomic charge of dyads **3**(**a**,**b**) and **4**(**a**,**b**)[a,b]

NBO	Dyads					
	3a	**4a**	**Δ4a,3a**[c]	**3b**	**4b**	**Δ4b,3b**
NI	0.108	0.222	0.113	0.141	0.232	0.090
Phenyl	0.008	0.031	0.023	−0.080	−0.032	0.047
Alkinyl	0.284	0.286	0.002	0.285	0.297	0.011
N4	−0.395	−0.279	0.115	−0.381	−0.282	0.099
N5	−0.249	−0.214	0.034	−0.208	−0.169	0.038
C6	0.011	0.220	0.209	−0.035	0.187	0.223
C11	−0.100	−0.091	0.009	−0.187	−0.172	0.015
C12	0.207	0.190	−0.016	0.197	0.185	−0.019
H9	0.397			0.400		
H10	0.193			0.220		
C44		−0.111			−0.111	
C45		0.111			0.111	
C6–N4	0.406	0.499	0.093	0.346	0.470	0.124
N5–N4	0.145	0.064	−0.081	0.173	0.052	−0.121
C6–C11	0.111	0.300	0.051	0.152	0.360	0.050
N5–C12	−0.456	−0.405	0.189	−0.405	−0.355	0.208

[a] In **4a** and **4b** the C44 and C45 represent two sp^3 carbon atom of C_{60}.
[b] The NBO of parent C_{60} is zero.
[c] **Δ4a**,**3a** represent the difference value between **4a** and **3a**.

These evidences indicated that charges in **4b** were transmitted to the pentafluorophenyl and C_{60} moiety that enhanced the charge-transfer interaction in the excited state; thus, the fluorescence intensity of **4b** was weaker than that of **4a**. This result was confirmed by fluorescence spectra.

3. Conclusion

Pz[60]–NI fluorescent derivatives functionalized with various substituents have been synthesized in one pot via a [3+2] dipolar cycloaddition between C_{60} and corresponding hydrazone. In this study, Pz[60]–NI provided a better fluorescence property than 4-aziridino[60]fullerene–1,8-naphthalimide (**5**); pyrazoline ring acted as a better bridge than aziridine in the PET processes. Electrochemical study revealed that Pz[60]–NI anodically shifted first reduction potential in comparison with the parent C_{60}, which indicated that Pz[60]–NI possess a better electron acceptor character than that of the parent C_{60}. Theoretical calculations were used to obtain optimized structures as well as spatial distributions of the HOMO and LUMO levels of the dyads **4**(**a**,**b**). The results suggest the existence of charge-separated states and the gap of HOMO–LUMO in **4a**–**e** were smaller than that in the parent C_{60}, which enables an easier electron-transfer process. The NBO of the dyads **4**(**a**,**b**) were calculated and it was found that the sp^3 nitrogen atom in the pyrazoline ring plays a key role in the charge transfer process.

4. Experimental section

4.1. General remarks

C_{60} was purchased from Wuhan University with 99% purity. Carbon disulfide, benzene, and toluene were used in AR quality.

Thin layer chromatography (TLC) was performed on a silica gel. All melting points were taken with a WRS-1 digital melting point apparatus made by Shanghai physical instrument factory (SPOIF), China. ^{1}H, ^{13}C, and ^{19}F NMR spectra were recorded on Bruker AV-500 spectrometer. Chemical shifts for ^{1}H NMR spectra were reported in parts per million downfield from TMS, chemical shifts for ^{13}C NMR spectra were reported in ppm relative to internal chloroform (δ 77.2 ppm for ^{13}C), and chemical shifts for ^{19}F NMR spectra were reported in ppm downfield from internal fluorotrichloromethane ($CFCl_3$). The terms m, s, d, t, q refer to multiple, singlet, doublet, triplet, and quarter, respectively. Infrared spectra (IR) were recorded with an AVATAR 370 FTIR spectrometer; the absorbance frequencies were given at maximum of intensity in cm^{-1}. High-resolution mass spectra were obtained with MicroMass Q-Tof Micro LC/MS and IonSpec 4.7 Tesla FTMS spectrometer. UV–vis absorption spectra were recorded on CRAY-100 spectrophotometer. Fluorescence measurements were carried out with Perkin–Elmer LS55 in a solution of 10^{-6} mol/L. Electrochemical measurements were performed using a Base 2000 CV system electrochemical analyzer. Cyclic voltammetric measurements were carried out in *o*-dichlorobenzene/acetonitrile (4:1) containing 0.1 M n-Bu_4NPF_6 as a supporting electrolyte, using a Pt working electrode (φ=1 mm) with ferrocene, and a vitreous carbon rod counter electrode, scan rate: 100 mV/s.

4.2. Synthesis

4.2.1. Preparation of hydrazones. **1** was prepared according to the published literature,[12] which served as the starting material for further synthesis. *2-Dodecyl-6-hydrazinyl-1H-benzo isoquinoline-1,3(2H)-dione* (**1**). Yield 89%. ^{1}H NMR ($CDCl_3$, δ): 8.61 (d, *J*=6.4 Hz, 1H), 8.55 (d, *J*=8.0 Hz, 1H), 8.04 (d, *J*=7.6 Hz, 1H), 7.67 (d, *J*=7.2 Hz, 2H), 6.58 (s, 1H), 4.17 (s, 2H), 3.51(s, 2H), 1.49–1.71(m, 20H), 0.97 (s, 3H).

A solution of the corresponding aldehyde **2a**–**k** (1.1 mmol), hydrazine **1** (1 mmol) and two drops of acetic acid in 20 mL of ethanol was heated under reflux for 1–2 h. The mixture was cooled to room temperature, filtered and the solid was recrystallized from acetone and ethanol mixture (4:1, *v*/*v*) to afford hydrazones **3**.

*4.2.1.1. N-Dodecyl-4-(benzylimino)amino-1,8-naphthalimide (**3a**).* Yield: 89%; mp 173–175 °C; IR (KBr) ν_{max} (cm^{-1}): 3441, 3266, 2922, 2851, 1702, 1690, 1661, 1586, 1390, 1355, 1241, 1112, 777, 753; ^{1}H NMR (500 MHz, $CDCl_3$, δ): 8.69 (s, 1H , NH), 8.62 (d, *J*=7 Hz, 1H), 8.58 (d, *J*=8.5 Hz, 1H), 8.20 (d, *J*=8.5 Hz, 1H), 8.07 (s, 1H), 7.84 (d, *J*=8.5 Hz, 1H), 7.78 (d, *J*=8.5 Hz, 2H), 7.69 (t, *J*=8.5 Hz, 1H), 7.41–7.47 (m, 3H), 4.16 (t, *J*=7.5 Hz, 2H), 1.69–1.75 (m, 2H), 1.24–1.35 (m, 18H), 0.87 (t, *J*=7.5 Hz, 3H); ^{13}C NMR (125 MHz, $CDCl_3$, δ): 164.34, 163.90, 142.97, 133.82, 131.16, 129.97, 128.91, 127.04, 125.33, 125.22, 108.44, 40.41, 31.94, 29.67, 29.65, 29.60, 29.45, 29.37, 28.23, 28.10, 27.23, 22.71, 14.15; EIMS (70 eV) *m*/*z*: 483.3 ([M]$^+$, 100); HRMS: calcd for $C_{31}H_{38}N_3O_2^{+1}$ [M+H]$^+$ 484.2968; found 484.2958.

*4.2.1.2. N-Dodecyl-4-(pentafluorobenzylimino)amino-1,8-naphthalimide (**3b**).* Yield: 87%; mp 145–146 °C; IR (KBr) ν_{max} (cm^{-1}): 3446, 3266, 2921, 2850, 1702, 1691, 1660, 1572, 1519, 1493, 1388, 1357, 1345, 1249, 1231, 966, 779; ^{1}H NMR (500 MHz, $CDCl_3$, δ): 9.03 (s, 1H, NH), 8.62 (d, *J*=7.5 Hz, 1H), 8.55–8.57 (m, 1H), 8.24 (d, *J*=8 Hz, 1H), 8.11 (s, 1H), 7.79 (d, *J*=8.5 Hz, 1H), 7.71 (t, *J*=8 Hz, 1H), 4.15 (t, *J*=8 Hz, 2H), 1.70–1.73 (m, 2H), 1.24 (s, 18H), 0.87–0.89 (m, 3H); ^{19}F NMR (470 MHz, $CDCl_3$, δ): −141.81–−141.87 (m, 2F), −152.40–−152.48 (m, 1F), −161.53–−161.63 (m, 2F); ^{13}C NMR (125 MHz, $CDCl_3$, δ): 164.34, 163.65, 143.69, 133.53, 133.23, 131.27, 131.10, 130.66, 130.20, 129.46, 128.09, 125.78, 125.17, 123.53, 123.20, 122.34, 118.97, 114.95, 109.28, 40.66, 31.93, 29.63, 29.56, 29.43, 29.37, 28.20, 28.10, 27.21, 27.14, 22.70, 14.13; EIMS (70 eV) *m*/*z*: 573.3 ([M]$^+$, 4); 553.3 ([M−F]$^+$, 100); HRMS: calcd for $C_{31}H_{33}N_3O_2F_5^{+1}$ [M+H]$^+$ 574.2502; found 574.2487.

*4.2.1.3. N-Dodecyl-4-(4-nitrobenzylimino)amino-1,8-naphthalimide (**3c**).* Yield: 87%; mp 160–162 °C; IR (KBr) ν_{max} (cm^{-1}): 3448, 2923, 2851, 1692, 1641,1586, 1389, 1339, 1278, 1241, 1124, 1104, 776; ^{1}H NMR (500 MHz, $CDCl_3$, δ): 8.95 (s, 1H, NH), 8.63 (d, *J*=8.5 Hz, 1H), 8.60 (d, *J*=8.5 Hz, 1H), 8.31 (d, *J*=8.5 Hz, 2H), 8.20 (d, *J*=8.5 Hz, 1H), 8.11 (s, 1H), 7.93 (d, *J*=7.5 Hz, 2H), 7.87 (d, *J*=7.5 Hz, 1H), 7.72–7.74 (m, 1H), 4.16 (s, 2H), 1.73 (s, 2H), 1.24 (s, 18H), 0.87 (s, 3H); ^{13}C NMR (125 MHz, $CDCl_3$, δ): 164.33, 163.92, 148.12, 143.88, 140.14, 139.55, 133.49, 131.30, 130.50, 129.51, 127.31, 125.77, 124.97, 124.11, 123.58, 119.01, 114.72, 109.10, 58.51, 40.47, 31.93, 29.63, 29.58, 29.42, 29.36, 28.20, 27.20, 22.70, 18.45, 14.13; EIMS (70 eV) *m*/*z*: 528.3 ([M]$^+$, 38); 379.3 ([$C_{24}H_{31}N_2O_2$]$^+$, 100); HRMS: calcd for $C_{31}H_{37}N_4O_4^{+1}$ [M+H]$^+$ 529.2823; found 529.2809.

*4.2.1.4. N-Dodecyl-4-(4-N,N dimethylaminobenzylimino)amino-1,8-naphthalimide (**3d**).* Yield: 86%; mp 194–196 °C; IR (KBr) ν_{max} (cm^{-1}): 3444, 3317, 3264, 2920, 2850, 1638, 1636, 1612, 1570, 1389, 1352, 1104, 775; ^{1}H NMR (500 MHz, $CDCl_3$, δ): 8.60 (d, *J*=8 Hz, 1H), 8.54 (d, *J*=8 Hz, 1H), 8.20 (d, *J*=8 Hz, 1H), 7.99 (s, 1H), 7.77 (d, *J*=8 Hz, 1H), 7.65 (d, *J*=9 Hz, 3H), 6.80 (s, 2H), 4.16 (t, *J*=7 Hz, 2H), 3.05 (s, 6H), 1.69–1.75 (m, 2H), 1.24 (s, 18H), 0.87 (t, *J*=7 Hz, 3H); ^{13}C NMR (125 MHz, $CDCl_3$, δ): 164.10, 163.95, 146.82, 133.94, 131.08, 129.69, 128.54, 125.66, 125.07, 123.25, 118.74, 111.02, 107.91, 40.73, 40.37, 40.10, 34.88, 31.93, 29.66, 29.60, 29.45, 29.37, 28.24, 27.24, 22.70, 18.44, 14.13; EIMS (70 eV) *m*/*z*: 526.4 ([M]$^+$, 100); HRMS: calcd for $C_{33}H_{42}N_4O_2Na^{+1}$ [M+Na+H]$^+$ 549.3185; found 549.3200.

*4.2.1.5. N-Dodecyl-4-(4-ethyloxybenzylimino)amino-1,8-naphthalimide (**3e**).* Yield: 88%; mp>200 °C; IR (KBr) ν_{max} (cm^{-1}): 3443, 3270, 2921, 2851, 1687, 1641, 1572, 1390, 1354, 1246, 1113, 1102, 775; ^{1}H NMR (500 MHz, $CDCl_3$ δ): 8.60 (d, *J*=7 Hz, 1H), 8.56 (d, *J*=8.5 Hz, 1H), 8.17–8.20 (m, 1H), 8.02 (s, 1H), 7.83 (d, *J*=8.5 Hz, 1H), 7.80 (d, *J*=8.5 Hz, 1H), 7.71 (d, *J*=8.5 Hz, 2H), 6.95–6.99 (m, 3H), 4.14–4.17 (m, 2H), 4.07–4.11 (m, 2H), 1.71–1.74 (m, 2H), 1.40–1.42 (m, 3H), 1.25 (s, 18H), 0.87–0.89 (m, 3H); ^{13}C NMR (125 MHz, $CDCl_3$, δ): 164.54, 164.07, 145.19, 143.22, 133.91, 131.08, 129.63, 128.60, 126.49, 125.34, 125.14, 123.34, 118.70, 114.87, 112.91, 108.09, 63.66, 40.38, 31.93, 31.43, 30.20, 29.71, 29.64, 29.44, 29.36, 28.23, 27.23, 22.70, 14.78, 14.13; EIMS (70 eV) *m*/*z*: 527.4 ([M]$^+$, 100); HRMS: calcd for $C_{33}H_{42}N_3O_3^{+1}$ [M+H]$^+$ 528.3226; found 528.3220.

*4.2.1.6. N-Dodecyl-4-(4-fluorobenzylimino)amino-1,8-naphthalimide (**3f**).* Yield: 85%; mp 157–159 °C; IR (KBr) ν_{max} (cm^{-1}): 3439, 2955, 2923, 2852, 1694, 1635, 1588, 1575, 1509, 1390, 1355, 1237, 1112, 775; ^{1}H NMR ($CDCl_3$): δ 8.67 (s, 1H, NH), 8.62 (d, *J*=7 Hz, 1H), 8.57 (d, *J*=8.5 Hz, 1H), 8.18 (d, *J*=8.5 Hz, 1H), 8.04 (s, 1H), 7.81 (d, *J*=8.5 Hz, 1H), 7.75–7.78 (m, 2H), 7.69 (t, *J*=8.5 Hz, 1H), 7.15 (t, *J*=8.5 Hz, 2H), 4.16 (t, *J*=7.5 Hz, 2H), 1.69–1.76 (m, 2H), 1.25 (s, 18H), 0.87 (t, *J*=7 Hz, 3H); ^{19}F NMR(470 MHz, $CDCl_3$, δ): −109.97–−110.01 (m, 1F); EIMS (70 eV) *m*/*z*: 501.4 ([M]$^+$, 89); 122.1 ([C_7H_5FN]$^+$, 100); HRMS: calcd for $C_{31}H_{37}N_3O_2F^{+1}$ [M+H]$^+$ 502.2883; found 502.2864.

*4.2.1.7. N-Dodecyl-4-(4-chlorobenzylimino)amino-1,8-naphthalimide (**3g**).* Yield: 90%; mp 173–174 °C; IR (KBr) ν_{max} (cm^{-1}): 3451, 3280, 2922, 2850, 1693, 1636, 1577, 1389, 1352, 1114, 1093, 774; ^{1}H NMR ($CDCl_3$, δ): 8.61 (d, *J*=7 Hz, 1H), 8.56 (d, *J*=8.5 Hz, 1H), 8.19 (d, *J*=8.5 Hz, 1H), 8.03 (s, 1H), 7.81 (d, *J*=8.5 Hz, 1H), 7.67–7.72 (m, 3H), 7.42 (d, *J*=8.5 Hz, 2H), 4.16 (t, *J*=7.5 Hz, 2H), 1.69–1.76 (m, 2H), 1.24 (s, 18H), 0.87 (t, *J*=7 Hz, 3H); EIMS (70 eV) *m*/*z*: 517.3 ([M]$^+$, 74); 379.3 ([$C_{24}H_{31}N_2O_2$]$^+$, 100); HRMS: calcd for $C_{31}H_{37}N_3O_2Cl^{+1}$ [M+H]$^+$ 518.2557; found 518.2568.

*4.2.1.8. N-Dodecyl-4-(4-bromobenzylimino)amino-1,8-naphthalimide (**3h**).* Yield: 86%; mp 171–172 °C; IR (KBr) ν_{max} (cm^{-1}): 3451, 3279, 2922, 2849, 1692, 1636, 1577, 1389, 1353, 1114, 775; ^1H NMR ($CDCl_3$, δ): 8.72 (s, 1H, NH), 8.56–8.62 (m, 2H), 8.18 (d, J=8.5 Hz, 1H), 8.02 (s, 1H), 7.81 (d, J=8.5 Hz, 1H), 7.57–7.69 (m, 5H), 4.15–4.16 (m, 2H), 1.71–1.72 (m, 2H), 1.24 (s, 18H), 0.87–0.89 (m, 3H); EIMS (70 eV) m/z: 561.2 ($[M]^+$, 79); 379.3 ($[C_{24}H_{31}N_2O_2]^+$, 100); HRMS: calcd for $C_{31}H_{37}N_3O_2Br^{+1}$ $[M+H]^+$ 562.2067; found 562.2063.

*4.2.1.9. N-Dodecyl-4-(2,4-difluorobenzylimino)amino-1,8-naphthalimide(**3i**).* Yield: 86%; mp 152–154 °C; IR (KBr) ν_{max} (cm^{-1}): 3450, 3282, 2923, 2852, 1689, 1637, 1613, 1574, 1389, 1354, 1116, 776; ^1H NMR ($CDCl_3$, δ): 8.89 (s, 1H, NH), 8.61 (d, J=7 Hz, 1H), 8.56 (d, J=8.5 Hz, 1H), 8.27 (s, 1H), 8.21 (d, J=8.5 Hz, 1H), 8.11 (dd, J=8.5, 15.5 Hz, 1H), 7.79 (d, J=8.5 Hz, 1H), 7.69 (t, J=8 Hz, 1H), 6.99 (t, J=8.5 Hz, 1H), 6.85–6.89 (m, 1H), 4.16 (t, J=7.5 Hz, 2H), 1.69–1.75 (m, 2H), 1.24 (s, 18H), 0.87 (t, J=7 Hz, 3H); ^{19}F NMR(470 MHz, $CDCl_3$, δ): −106.52−−106.57 (m, 1F), −117.24−−117.29 (m, 1F); EIMS (70 eV) m/z: 519.2 ($[M]^+$, 44); 365.3 ($[C_{24}H_{30}NO_2]^+$, 100); HRMS: calcd for $C_{31}H_{36}N_3O_2F_2^{+1}$ $[M+H]^+$ 520.2788; found 520.2770.

*4.2.1.10. N-Dodecyl-4-(4-nitrilebenzylimino)amino-1,8-naphthalimide (**3j**).* Yield: 89%; mp 189–191 °C; IR (KBr) ν_{max} (cm^{-1}): 3441, 2921, 2851, 2222, 1692, 1648, 1576, 1388, 1358, 1241, 1120, 1102, 775; ^1H NMR ($CDCl_3$, δ): 9.07 (s, 1H, NH), 8.56–8.61 (m, 2H), 8.19–8.24 (m, 1H), 8.08 (s, 1H), 7.82–7.86 (m, 2H), 7.69–7.77 (m, 4H), 4.15–4.18 (m, 2H), 1.70–1.73 (m, 2H), 1.24 (s, 18H), 0.87–0.89 (m, 3H); EIMS (70 eV) m/z: 508.2 ($[M]^+$, 38); 379.3 ($[C_{24}H_{31}N_2O_2]^+$, 100); HRMS: calcd for $C_{32}H_{37}N_4O_2^{+1}$ $[M+H]^+$ 509.2909; found 509.2911.

*4.2.1.11. N-Dodecyl-4-(4-formylbenzylimino)amino-1,8-naphthalimide (**3k**).* Yield: 85%; mp 144–146 °C; IR (KBr) ν_{max} (cm^{-1}): 3451, 3312, 2923, 2851, 1690, 1643, 1579, 1548, 1390, 1355, 1260, 1118, 1099, 1020, 804, 775; ^1H NMR ($CDCl_3$, δ): 10.06 (s, 1H), 8.92 (s, 1H, NH), 8.63 (d, J=7 Hz, 1H), 8.59 (d, J=8.5 Hz, 1H), 8.22 (d, J=8.5 Hz, 1H), 8.11 (s, 1H), 7.94 (dd, J=8.5, 16 Hz, 4H), 7.87 (d, J=8.5 Hz, 1H), 7.71 (t, J=8.5 Hz, 1H), 4.16 (t, J=8 Hz, 2H), 1.70–1.76 (m, 2H), 1.25 (s, 18H), 0.87–0.89 (m, 3H); EIMS (70 eV) m/z: 511.3 ($[M]^+$, 91); 379.2 ($[C_{24}H_{31}N_2O_2]^+$, 100); HRMS: calcd for $C_{32}H_{38}N_3O_3^{+1}$ $[M+H]^+$ 512.2904; found 512.2907.

4.2.2. Typical procedure for the synthesis of fulleropyrazolines. Under nitrogen atmosphere a mixture of C_{60} (72 mg, 0.1 mmol), hydrazones **3** (0.2 mmol), and $PhI(OAc)_2$ (64 mg, 0.2 mmol) was dissolved in 40 mL of benzene and stirred at 40 °C for a desired time. The solvent was then evaporated in vacuo and the residue was separated on a silica gel column using CS_2 or CS_2–toluene as the eluent to afford unreacted C_{60} and adduct **4**.

*4.2.2.1. 1′-(N-Dodecyl-1,8-naphthalimidyl)-3′-(phenyl)pyrazolino [60]fullerene (**4a**).* Brown solid, Yield: 29.2 mg (24%, 81% based on reacted C_{60}); IR (KBr) ν_{max} (cm^{-1}): 3449, 2963, 2924, 2848, 1699, 1657, 1494, 1460, 1413, 1261, 1096, 1021, 865, 801, 702, 525; ^1H NMR (500 MHz, $CDCl_3$, δ): 9.14 (d, J=8 Hz, 1H), 8.74 (d, J=8 Hz, 1H), 8.66 (d, J=7.5 Hz, 1H), 8.33 (d, J=7.5 Hz, 2H), 8.27 (d, J=8 Hz, 1H), 7.83 (t, J=8 Hz, 1H), 7.52–7.55 (m, 3H), 4.17 (t, J=7.5 Hz, 2H), 1.72–1.73 (m, 2H), 1.25 (s, 18H), 0.87–0.89 (m, 3H); ^{13}C NMR (125 MHz, $CDCl_3$, δ): 164.14, 163.80, 147.67, 147.24, 146.91, 146.40, 146.26, 146.01, 145.85, 145.59, 145.27, 144.97, 144.36, 144.26, 144.15, 143.15, 142.93, 142.41, 142.26, 142.13, 142.11, 141.88, 140.42, 138.54, 136.41, 135.96, 131.88, 130.01, 129.96, 129.04, 128.88, 127.11, 126.87, 124.48, 123.99, 123.15, 119.11, 60.42, 58.50, 40.65, 34.88, 31.92, 31.44, 30.19, 29.63, 29.16, 28.16, 27.19, 22.69, 18.44, 14.15; ESI-MS: calcd for $C_{91}H_{35}N_3O_2$: 1202.27; found 1201.95 $[(M-H)^-]$.

*4.2.2.2. 1′-(N-Dodecyl-1,8-naphthalimidyl)-3′-(2,3,4,5,6-pentafluorophenyl)pyrazolino-[60]fullerene (**4b**).* Brown solid, Yield: 36.8 mg (21%, 83% based on reacted C_{60}); IR (KBr) ν_{max} (cm^{-1}): 3445, 2961, 2921, 2850,1701, 1662, 1494, 1261, 1098, 1022, 801, 526; ^1H NMR (500 MHz, $CDCl_3$, δ): 9.10 (d, J=8.5 Hz, 1H), 8.75 (d, J=7.5 Hz, 1H), 8.69 (d, J=6.5 Hz, 1H), 8.25 (d, J=8 Hz, 1H), 7.89 (t, J=8.5 Hz, 1H), 4.17 (t, J=7.5 Hz, 2H), 1.70–1.76 (m, 2H), 1.25 (s, 18H), 0.86 (t, J=7 Hz, 3H); ^{19}F NMR (470 MHz, $CDCl_3$, δ): −135.99−−136.03 (m, 2F), −148.70−−148.79 (m, 1F); −159.07−−159.17 (m, 2F); ^{13}C NMR (125 MHz, $CDCl_3$, δ): 164.03, 163.61, 147.79, 147.31, 146.38, 146.09, 145.99, 145.61, 145.51, 145.43, 145.27, 144.70, 144.35, 144.28, 144.03, 143.17, 142.90, 142.81, 142.28, 142.15, 141.97, 141.02, 137.89, 136.30, 131.96, 131.31, 129.81, 128.24, 127.50, 126.81, 125.31, 123.26, 122.34, 92.28, 58.51, 40.69, 34.54, 31.93, 30.19, 29.72, 29.57, 29.36, 28.16, 27.19, 22.70, 18.46, 14.15; ESI-MS: calcd for $C_{91}H_{30}F_5N_3O_2$: 1292.22; found 1292.32 $[(M-H)^-]$.

*4.2.2.3. 1′-(N-Dodecyl-1,8-naphthalimidyl)-3′-(4-nitrophenyl) pyrazolino[60]fullerene (**4c**).* Brown solid, Yield: 27.5 mg (23%, 85% based on reacted C_{60}); IR (KBr) ν_{max} (cm^{-1}): 3443, 2960, 2919, 2848, 1699, 1659, 1583, 1338, 1261, 1101, 1025, 849, 802, 526; ^1H NMR (500 MHz, $CDCl_3$, δ): 9.02 (d, J=9 Hz, 1H), 8.74 (d, J=8 Hz, 1H), 8.69 (d, J=7 Hz, 1H), 8.60 (d, J=9 Hz, 2H), 8.40 (d, J=9 Hz, 2H), 8.27 (d, J=8 Hz, 1H), 7.87 (t, J=8 Hz, 1H), 4.18 (t, J=7.5 Hz, 2H), 1.72–1.74 (m, 2H), 1.25 (s, 18H), 0.85–0.87 (m, 3H); ^{13}C NMR (125 MHz, $CDCl_3$, δ): 163.97, 163.58, 148.01, 147.71, 147.33, 146.46, 146.33, 146.10, 146.07, 145.94, 145.66, 145.52, 145.44, 145.34, 145.27, 144.84, 144.22, 144.16, 144.12, 143.16, 143.02, 142.42, 142.21, 140.51, 138.38, 135.96, 131.97, 131.24, 130.12, 129.11, 127.54, 124.26, 123.34, 122.43, 112.97, 93.51, 80.34, 40.70, 31.94, 29.72, 29.67, 29.63, 29.58, 29.41, 29.38, 28.17, 27.19, 22.71, 14.15; ESI-MS: calcd for $C_{91}H_{34}N_4O_4$: 1247.27; found 1247.28 $([M-H]^-)$.

*4.2.2.4. 1′-(N-Dodecyl-1,8-naphthalimidyl)-3′-(4-dimethylaminophenyl)pyrazolino-[60]fullerene (**4d**).* Brown solid, Yield: 27.8 mg (22%, 70% based on reacted C_{60}); IR (KBr) ν_{max} (cm^{-1}): 3438, 2959, 2923, 2850, 1700, 1664, 1602, 1589, 1376, 1351, 1261, 1173, 1096, 1021, 803, 594; ^1H NMR (500 MHz, $CDCl_3$, δ): 9.16 (d, J=8 Hz, 1H), 8.70 (d, J=9 Hz, 2H), 7.97–7.99 (m, 3H), 7.89 (t, J=8 Hz, 1H), 6.73 (d, J=9 Hz, 2H), 4.17 (t, J=7.5 Hz, 2H), 3.13 (s, 6H), 1.74–1.77 (m, 2H), 1.25 (s, 18H), 0.86–0.88 (m, 3H); ESI-MS: calcd for $C_{93}H_{40}N_4O_2$: 1245.34; found 1244.84 $([M-H]^-)$.

*4.2.2.5. 1′-(N-Dodecyl-1,8-naphthalimidyl)-3′-(4-ethyoxylphenyl) pyrazolino[60]fullerene (**4e**).* Brown solid, Yield: 25.9 mg (21%, 67% based on reacted C_{60}); IR (KBr) ν_{max} (cm^{-1}): 3459, 2962, 2923, 2852, 1699, 1659, 1587, 1494, 1461, 1400, 1261, 1096, 1021, 801, 702, 526; ^1H NMR (500 MHz, $CDCl_3$, δ): 9.16 (d, J=8.5 Hz, 1H), 8.74 (d, J=7.5 Hz, 1H), 8.65 (d, J=7.5 Hz, 1H), 8.25–8.28 (m, 3H), 7.81 (t, J=7.5 Hz, 1H), 7.54 (d, J=8.5 Hz, 2H), 4.18 (t, J=7 Hz, 2H), 4.12(q, J=3 Hz, 2H), 1.72–1.75 (m, 2H), 1.41–1.43 (m, 3H), 1.26 (s, 18H), 0.87–0.88 (m, 3H); ^{13}C NMR (125 MHz, $CDCl_3$, δ): 164.16, 163.78, 147.64, 147.45, 146.39, 146.05, 145.83, 145.59, 145.50, 145.39, 145.20, 144.39, 144.17, 143.14, 142.92, 142.40, 142.11, 140.39, 139.75, 136.39, 135.94, 134.36, 132.01, 131.45, 129.98, 129.75, 129.04, 127.83, 126.99, 126.75, 125.31, 124.09, 123.11, 119.12, 114.73, 92.89, 81.48, 63.92, 58.47, 40.65, 34.88, 34.53, 31.44, 30.20, 29.66, 29.36, 28.17, 27.20, 22.70, 18.43, 14.79, 14.13; ESI-MS: calcd for $C_{93}H_{39}N_3O_3$: 1246.32; found 1246.14 $([M-H]^-)$.

*4.2.2.6. 1′-(N-Dodecyl-1,8-naphthalimidyl)-3′-(4-fluorophenyl) pyrazolino[60]fullerene (**4f**).* Brown solid, Yield: 28.3 mg (23%, 83% based on reacted C_{60}); IR (KBr) ν_{max} (cm^{-1}): 3449, 2962, 2919, 2849, 1699, 1659, 1587, 1350, 1261, 1096, 1023, 802, 526; ^1H NMR (500 MHz, $CDCl_3$, δ): 9.11 (d, J=8.5 Hz, 1H), 8.73 (d, J=8 Hz, 1H), 8.66 (d, J=7 Hz, 1H), 8.60(d, J=8 Hz, 1H), 8.31–8.34 (m, 2H), 8.25 (d,

J=8 Hz, 1H), 8.21 (d, *J*=8 Hz, 1H), 7.82 (t, *J*=8 Hz, 1H), 4.17 (t, *J*=7.5 Hz, 2H), 1.71–1.74 (m, 2H), 1.25 (s, 18H), 0.87–0.88 (m, 3H); ^{19}F NMR(470 MHz, $CDCl_3$, δ): −109.87––109.93 (m, 1F); ESI-MS: calcd for $C_{91}H_{34}FN_3O_2$: 1220.26; found 1220.37 ([M−H]$^-$).

*4.2.2.7. 1′-(N-Dodecyl-1,8-naphthalimidyl)-3′-(4-chlorophenyl) pyrazolino[60]fullerene (**4g**).* Brown solid, Yield: 33.6 mg (27%, 85% based on reacted C_{60}); IR (KBr) ν_{max} (cm^{-1}): 3451, 2919, 2848, 1699, 1659, 1585, 1384, 1351, 1260, 1094, 804, 783, 526; ^{1}H NMR (500 MHz, $CDCl_3$, δ): 9.09 (d, *J*=8.5 Hz, 1H), 8.73 (d, *J*=8 Hz, 1H), 8.66 (d, *J*=7.5 Hz, 1H), 8.29 (d, *J*=9 Hz, 2H), 8.25 (d, *J*=8 Hz, 1H), 7.83 (t, *J*=7.5 Hz, 1H), 7.52 (d, *J*=9 Hz, 2H), 4.17 (t, *J*=7.5 Hz, 2H), 1.71–1.74 (m, 2H), 1.24–1.26 (m, 18H), 0.85–0.87 (m, 3H); ESI-MS: calcd for $C_{91}H_{34}ClN_3O_2$: 1236.72; found 1236.45 ([M−H]$^-$).

*4.2.2.8. 1′-(N-Dodecyl-1,8-naphthalimidyl)-3′-(4-bromophenyl) pyrazolino[60]fullerene (**4h**).* Brown solid, Yield: 37.4 mg (29%, 86% based on reacted C_{60}); IR (KBr) ν_{max} (cm^{-1}): 3446, 2919, 2848, 1699, 1659, 1584, 1384, 1351, 1260, 1235, 1098, 1074, 822, 782, 526; ^{1}H NMR (500 MHz, $CDCl_3$, δ): 9.09 (d, *J*=8.5 Hz, 1H), 8.73 (d, *J*=8 Hz, 1H), 8.66 (d, *J*=7.5 Hz, 1H), 8.23 (t, *J*=9 Hz, 3H), 7.83 (t, *J*=8 Hz, 1H), 7.68 (d, *J*=8.5 Hz, 2H), 4.17 (t, *J*=7.5 Hz, 2H), 1.70–1.76 (m, 2H), 1.25 (s, 18H), 0.83–0.86 (m, 3H); ESI-MS: calcd for $C_{91}H_{34}BrN_3O_2$: 1281.17; found 1281.33 ([M−H]$^-$).

*4.2.2.9. 1′-(N-Dodecyl-1,8-naphthalimidyl)-3′-(2,4-difluorophenyl)pyrazolino[60]fullerene (**4i**).* Brown solid, Yield: 29.4 mg (24%, 82% based on reacted C_{60}); IR (KBr) ν_{max} (cm^{-1}): 3442, 2962, 2922, 2850, 1698, 1658, 1587, 1261, 1096, 1022, 866, 801, 702, 525; ^{1}H NMR (500 MHz, $CDCl_3$, δ): 9.18 (dd, *J*=1, 8.5 Hz, 1H), 8.74 (d, *J*=7.5 Hz, 1H), 8.66 (d, *J*=6.5 Hz, 1H), 8.61 (dd, *J*=1, 7 Hz, 1H), 8.27 (d, *J*=7.5 Hz, 1H), 8.21 (d, *J*=7.5 Hz, 1H), 7.95 (dd, *J*=8.5, 14.5 Hz, 1H), 7.86 (t, *J*=7.5 Hz, 1H), 4.15–4.18 (m, 2H), 1.70–1.74 (m, 2H), 1.25 (s, 18H), 0.86–0.87 (m, 3H); ^{19}F NMR (470 MHz, $CDCl_3$, δ): −105.39––105.46 (m, 1F), −106.59––106.64 (m, 1F); ^{13}C NMR (125 MHz, $CDCl_3$, δ): 164.24, 163.73, 147.71, 147.24, 146.71, 146.37, 146.04, 145.93, 145.50, 145.38, 145.25, 144.37, 144.21, 144.06, 143.21, 143.14, 142.88, 142.29, 142.23, 142.18, 142.05, 141.92, 140.75, 139.77, 136.29, 133.85, 131.90, 131.60, 131.20, 129.82, 128.18, 126.94, 123.14, 122.79, 121.85, 119.88, 92.14, 82.39, 40.54, 31.93, 29.71, 29.64, 29.57, 29.41, 29.36, 28.16, 27.18, 22.70, 18.45, 14.14; ESI-MS: calcd for $C_{91}H_{33}F_2N_3O_2$: 1238.25; found 1238.36 ([M−H]$^-$).

*4.2.2.10. 1′-(N-Dodecyl-1,8-naphthalimidyl)-3′-(4-cyanophenyl) pyrazolino[60]fullerene (**4j**).* Brown solid, Yield: 30.4 mg (25%, 80% based on reacted C_{60}); IR (KBr) ν_{max} (cm^{-1}): 3447, 2920, 2849, 2226 (−CN), 1701, 1661, 1587,1352, 1236, 1102, 784, 527; ^{1}H NMR (500 MHz, $CDCl_3$, δ): 9.03 (d, *J*=8.5 Hz, 1H), 8.73 (d, *J*=7.5 Hz, 1H), 8.68 (d, *J*=6.5 Hz, 1H), 8.53 (d, *J*=8.5 Hz, 2H), 8.26 (d, *J*=8 Hz, 1H), 7.86 (t, *J*=8 Hz, 1H), 7.83 (d, *J*=8.5 Hz, 2H), 4.17(t, *J*=7.5 Hz, 2H), 1.71–1.73 (m, 2H), 1.25 (s, 18H), 0.83–0.85 (m, 3H); ^{13}C NMR (125 MHz, $CDCl_3$, δ): 164.00, 163.61, 147.71, 147.33, 146.46, 146.32, 146.08, 145.92, 145.64, 145.53, 145.48, 145.34, 145.27, 144.95, 144.24, 143.64, 143.23, 142.91, 142.41, 142.28, 142.18, 142.04, 141.92, 140.50, 140.03, 136.67, 136.53, 135.94, 132.73, 131.95, 130.10, 128.91, 127.47, 123.30, 122.33, 112.97, 93.44, 40.70, 31.93, 29.66, 29.64, 29.57, 29.40, 29.36, 29.07, 28.16, 27.18, 22.70, 14.15; ESI-MS: calcd for $C_{92}H_{34}N_4O_2$: 1227.28; found 1226.07 ([M−H]$^-$).

*4.2.2.11. 1′-(N-Dodecyl-1,8-naphthalimidyl)-3′-(4-formylphenyl) pyrazolino[60]fullerene (**4k**).* Brown solid, Yield: 26.8 mg (22%, 66% based on reacted C_{60}); IR (KBr) ν_{max} (cm^{-1}): 3443, 2954, 2921, 2850, 1700, 1659, 1585, 1462, 1356, 1261, 1100, 1027, 804, 784, 526; ^{1}H NMR (500 MHz, $CDCl_3$, δ): 10.10 (s, 1H), 9.07 (dd, *J*=1, 8.5 Hz, 1H), 8.74 (d, *J*=8 Hz, 1H), 8.68 (dd, *J*=1, 7 Hz, 1H), 8.57 (d, *J*=8 Hz, 2H), 8.28 (d, *J*=8 Hz, 1H), 8.05 (d, *J*=8 Hz, 2H), 7.86 (t, *J*=8 Hz, 1H), 4.18 (t, *J*=7.5 Hz, 2H), 1.70–1.75 (m, 2H), 1.25 (s, 18H), 0.86–0.87 (m, 3H); ESI-MS: calcd for $C_{92}H_{35}N_3O_3$: 1230.28; found 1230.39 ([M−H]$^-$).

Acknowledgements

This work was supported by the National Natural Science Foundation of China (Nos. 20972092, 21032006, 21072216); MOST (2011BAE06B05). The authors thank the instrumental analysis & research center of Shanghai University and Dr. Hongmei Deng, High Performance Computing and Data Center, Shanghai Advanced Research Institute, Chinese Academy of Sciences.

Supplementary data

Supplementary data related to this article can be found at http://dx.doi.org/10.1016/j.tet.2012.08.031.

References and notes

1. (a) Brabec, C. J.; Sariciftci, N. S.; Hummelen, J. C. *Adv. Funct. Mater.* **2001**, *11*, 15–26; (b) Wudl, F. *Mater. Chem.* **2002**, *12*, 1959–1963; (c) Nierengarten, J.-F. *Sol. Energy Mater. Sol. Cells* **2004**, *83*, 187–199.
2. (a) Gust, D.; Moore, T. A.; Moore, A. L. *Acc. Chem. Res.* **2001**, *34*, 40–48; (b) Liu, H. B.; Xu, J. L.; Li, Y. J.; Li, Y. L. *Acc. Chem. Res.* **2010**, *43*, 1496–1508.
3. Echegoyen, L.; Echegoyen, L. E. *Acc. Chem. Res.* **1998**, *31*, 593–601.
4. (a) Guldi, D. M. *Chem. Soc. Rev.* **2002**, *31*, 22–36; (b) Verhoeven, J. W. *J. Photochem. Photobiol., C* **2006**, *7*, 40–60; (c) Xiao, S. Q.; Li, Y. L.; Li, Y. J.; Zhuang, J. P.; Wang, N.; Liu, H. B.; Ning, B.; Liu, Y.; Lu, F. S.; Fan, L. Z.; Yang, C. H.; Li, Y. F.; Zhu, D. B. *J. Phys. Chem. B* **2004**, *108*, 16677–16685; (d) Xiao, S. Q.; El-Khouly, M. E.; Li, Y. L.; Gan, Z. H.; Liu, H. B.; Jiang, L.; Araki, Y. Y.; Ito, O.; Zhu, D. B. *J. Phys. Chem. B* **2005**, *109*, 3658–3667; (e) Li, Y. J.; Wang, N.; He, X. R.; Wang, S.; Liu, H. B.; Li, Y. L.; Li, X. F.; Zhuang, J. P.; Zhu, D. B. *Tetrahedron* **2005**, *61*, 1563–1569.
5. Zhu, B.; Wang, G.-W. *Org. Lett.* **2009**, *11*, 4334.
6. Li, F.-B.; You, X.; Wang, G.-W. *Org. Lett.* **2010**, *12*, 4896.
7. (a) Langa, F.; Gómez-Escalonilla, M. J.; Rueff, J.-M.; Figueira Duarte, T. M.; Nierengarten, J.-F.; Palermo, V.; Samori, P.; Rio, Y.; Accorsi, G.; Armaroli, N. *Chem.—Eur. J.* **2005**, *11*, 4405–4415; (b) Accorsi, G.; Armaroli, N.; Eckert, J.-F.; Nierengarten, J.-F. *Tetrahedron Lett.* **2002**, *43*, 65–68; (c) de la Cruz, P.; Espíldora, E.; García, J. J.; de la Hoz, A.; Langa, F.; Martín, N.; Sánchez, L. *Tetrahedron Lett.* **1999**, *40*, 4889–4892.
8. (a) Armaroli, N.; Accorsi, G.; Gisselbrecht, J.-P.; Gross, M.; Krasnikov, V.; Tsamouras, D.; Hadziioannou, G.; Gómez-Escalonilla, M. J.; Langa, F.; Eckert, J.-F.; Nierengarten, J.-F. *J. Mater. Chem.* **2002**, *12*, 2077–2087; (b) de la Cruz, P.; Díaz-Ortiz, A.; García, J. J.; Gómez-Escalonilla, M. J.; de la Hoz, A.; Langa, F. *Tetrahedron Lett.* **1999**, *40*, 1587–1590.
9. (a) Oviedo, J. J.; El-Khouly, M. E.; de la Cruz, P.; Orduna, J.; Araki, Y.; Langa, F.; Ito, O. *New J. Chem.* **2006**, *30*, 93–101; (b) Langa, F.; Gómez-Escalonilla, M. J.; Diez-Barra, E.; García-Martínez, J. C.; de la Hoz, A.; Rodríguez-López, J.; González-Cortes, A.; López-Arza, V. *Tetrahedron Lett.* **2001**, *42*, 3435–3438; (c) Espíldora, E.; Delgado, J. L.; de la Cruz, P.; de la Hoz, A.; López-Arza, V.; Langa, F. *Tetrahedron* **2002**, *58*, 5821–5826.
10. (a) Wang, X.; Perzon, E.; Delgado, J. L.; de la Cruz, P.; Zhang, F.; Langa, F.; Andersson, M.; Inganäs, O. *Appl. Phys. Lett.* **2004**, *85*, 5081–5083; (b) Wang, X.; Perzon, E.; Oswald, F.; Langa, F.; Admassie, S.; Andersson, M.; Inganäs, O. *Adv. Funct. Mater.* **2005**, *15*, 1665–1670; (c) Gómez-Escalonilla, M. J.; Langa, F.; Rueff, J.-M.; Oswald, L.; Nierengarten, J.-F. *Tetrahedron Lett.* **2002**, *43*, 7507–7511.
11. Liu, F. R.; Du, W. Q.; Liang, Q.; Wang, Y. Q.; Zhang, J. M.; Zhao, J. W.; Zhu, S. Z. *Tetrahedron* **2010**, *66*, 5467–5471.
12. (a) Tian, H.; Xu, T.; Zhao, Y. B.; Chen, K. C. *J. Chem. Soc., Perkin Trans. 1* **1999**, *2*, 545–549; (b) Hasharoni, K.; Levanon, H.; Greefield, S. R.; Gosztola, D. J.; Svec, W. A.; Wasielewski, M. R. *J. Am. Chem. Soc.* **1996**, *118*, 10228.
13. Poteau, X.; Brown, A. I.; Brown, R. G.; Holmes, C.; Matthew, D. *Dyes Pigments* **2000**, *47*, 91.
14. (a) Gan, J. A.; Tian, H.; Wang, Z. H.; Chen, K. C.; Hill, J.; Lane, P. A.; Rahn, M. D.; Fox, A. M.; Bradley, D. D. C. *J. Organomet. Chem.* **2002**, *647*, 168–175; (b) Gunnlaugsson, T.; Kruger, P. E.; Jensen, P.; Tierney, J.; Ali, H. D. P.; Hussey, G. M. *J. Org. Chem.* **2005**, *70*, 10875–10878.
15. Yang, H. T.; Ruan, X. J.; Miao, C. B.; Sun, X. Q. *Tetrahedron Lett.* **2010**, *51*, 6056–6059.
16. Perdew, J.; Burke, K.; Parr, R. *Phys. Rev. B* **1988**, *37*, 785–789.
17. Ditchfield, R.; Hehre, W. J.; Pople, J. A. *J. Chem. Phys.* **1971**, *54*, 724–728.
18. Perez, L.; El-Khouly, M. E.; de la Cruz, P.; Araki, Y.; Ito, O.; Langa, F. *Eur. J. Org. Chem.* **2007**, 2175–2185.